Transp Porous Med (2009) 78:525–536
DOI 10.1007/s11242-008-9322-9

Stability of Thermosolutal Natural Convection in Superposed Fluid and Porous Layers

S. C. Hirata · B. Goyeau · D. Gobin

Received: 16 December 2007 / Accepted: 13 December 2008 / Published online: 13 January 2009

Abstract This article deals with the onset of thermosolutal natural convection in horizontal superposed fluid and porous layers. A linear stability analysis is performed using the one-domain approach. As in the thermal convection case, the results show a bimodal nature of the marginal stability curves where each mode corresponds to a different convective instability. At small wave numbers, the convective flow occurs in the whole cavity ("porous mode") while perturbations of large wave numbers lead to a convective flow mainly confined in the fluid layer ("fluid mode"). Furthermore, it is shown that the onset of thermosolutal natural convection is characterized by a multi-cellular flow in the fluid region for negative thermal Rayleigh numbers. For positive thermal Rayleigh numbers, the convective flow takes place both in the fluid and porous regions. The influence of the depth ratio and thermal diffusivity ratio is also investigated for a wide range of the thermal Rayleigh numbers.

Keywords Stability analysis · Thermosolutal natural convection · Fluid–porous interface

1 Introduction

Transport phenomena at the interface between a fluid and a porous layer is encountered in a wide range of industrial applications (multi-component solidification, thermal insulation, drying processes,. . .) or in the environment (benthic boundary layers, ground water pollution,. . .). In many of these situations, thermal and/or solutal natural convection is involved

S. C. Hirata · D. Gobin
Laboratoire FAST, Université Paris 6, UMR CNRS 7608, Bât. 502 Campus Universitaire, 91405 Orsay Cedex, France
e-mail: silvia@fast.u-psud.fr

D. Gobin
e-mail: gobin@fast.u-psud.fr

B. Goyeau (✉)
Laboratoire EM2C, UPR CNRS 288, Ecole Centrale Paris, 92295 Châtenay-Malabry Cedex 9, France
e-mail: benoit.goyeau@em2c.ecp.fr

and therefore the stability analysis for the onset of such convective flows has been the subject of particular attention since the pioneering study performed by Nield (1977). The large majority of stability analyses have been carried out using a two-domain approach. In that case, conservation equations in the fluid and porous regions are coupled by interfacial boundary conditions which can depend on the order of the partial differential equations. Indeed, for momentum transport, most of the studies uses Darcy's law in the porous region and Navier-Stokes equations in the fluid region Nield (1977, 1983), Chen and Chen (1988), Carr and Straughan (2003), Carr (2004). Under these circumstances, the coupling between the two homogeneous regions is obtained using a slip boundary condition Beavers and Joseph (1967) where the slip coefficient depends on the local nature and position of the interface Beavers et al. (1970). In both thermal and thermosolutal convective cases, the results using this modeling approach show a bimodal nature of the marginal stability curves where each mode corresponds to a different mode of convective instability Chen and Chen (1988). At small wave numbers the convective flow occurs in the whole cavity ("porous mode") while perturbations of large wave numbers lead to a convective flow mainly confined in the fluid layer ("fluid mode"). Another two-domain approach consists in using the Brinkman correction in Darcy's law allowing to satisfy the continuity of both velocity and stress at the fluid/porous interface (Brinkman 1947; Neale and Nader 1974). Only one stability analysis has been performed using this modeling. The comparison with the results obtained using the Beavers and Joseph condition (Beavers and Joseph 1967) shows a quantitative agreement depending on the values of the slip coefficient (Hirata et al. 2007b). Using a volume averaging method, an improvement of the momentum transport description at the fluid/porous interface has been proposed by deriving a stress jump boundary condition (Ochoa-Tapia and Whitaker 1995a,b). This latter condition involves a jump coefficient β which is explicitly dependent on the continuous spatial variations of the effective properties (porosity, permeability) at the fluid-porous inter-region (Goyeau et al. 2003; Chandesris and Jamet 2006). It has been recently obtained that the jump coefficient strongly influences the bimodal marginal stability curves giving rise to more unstable situations (Hirata et al. 2007a). Finally, an alternative modeling approach to describe heat and mass transport in a partially porous domain is the one-domain approach (Arquis and Caltagirone 1984). The porous layer is viewed as a pseudo-fluid and the whole cavity is treated as a continuum. In that case, heat and mass transport are governed by a unique set of conservation equations both valid in the fluid and porous regions avoiding the explicit formulation of the boundary conditions at the interface. Very few stability analyses have been performed using the one-domain approach (Zhao and Chen 2001). The comparisons with the two-domain models lead to a qualitative agreement of the marginal stability curves for the thermal case (bimodal behavior) whereas only the "fluid mode" was observed for the thermosolutal case. In both cases, the critical values of the thermal or solutal Rayleigh numbers may significantly differ (Zhao and Chen 2001; Chen and Chen 1988). Actually, in this formulation the macroscopic properties of the homogeneous porous layer at the interface (porosity, permeability, effective diffusivity) are Heaviside functions and therefore, their differentiation must be taken in the meaning of distributions (Schwartz 1961; Kataoka 1986). In that case, the one- and the two-domain approaches are shown to be equivalent, and very good agreement is indeed found when comparing the results obtained with both approaches (Hirata et al. 2009).

The objective of this article is to study the onset of thermosolutal natural convection in superposed fluid and porous layers with the one-domain model (with the derivatives in the sense of distributions). A linear stability analysis is carried out, and the resulting eigenvalue problem is solved using the Generalized Integral Transform Technique (GITT) (Cotta 1993). The critical solutal Rayleigh number is obtained for a wide range of thermal Rayleigh

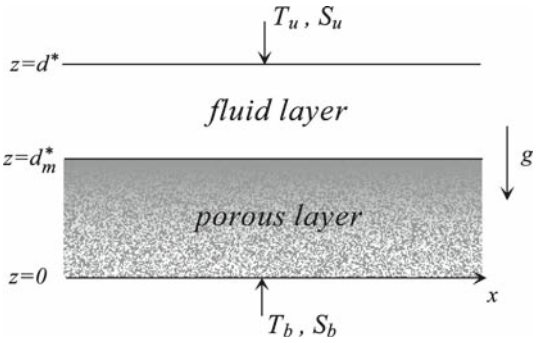

Fig. 1 Geometric configuration of the problem

numbers corresponding to stabilizing or destabilizing temperature gradients. The influence of the depth ratio and of the thermal diffusivity ratio is also investigated.

2 Mathematical Modeling

The geometrical configuration is composed by an infinite horizontal porous layer of thickness d_{m}^* underlying a fluid layer of thickness $d_{\mathrm{f}}^* = d^* - d_{\mathrm{m}}^*$ (Fig. 1). The porous layer is assumed to be homogeneous, isotropic and saturated by the overlying fluid which is assumed to be Newtonian and to satisfy the linear Boussinesq approximation. Therefore, the variations of the density $\rho(T, S)$ with temperature T and solute concentration S is given by $\rho(T, S) = \rho_0(1 - \beta_{\mathrm{T}}(T - T_0) - \beta_{\mathrm{S}}(S - S_0))$ where $\rho_0 = \rho(T_0, S_0)$ and where β_{T} and β_{S} are the thermal and solutal expansion coefficients, respectively. For the analysis of the results presented in Sect. 4, it is important to recall that $\beta_{\mathrm{T}} \geq 0$ while $\beta_{\mathrm{S}} \leq 0$. The horizontal walls are impermeable and are maintained at different temperatures and concentrations: T_{u}, S_{u} (top) and T_{b}, S_{b} (bottom).

As previously mentioned, the one-domain approach has been chosen in this analysis.The dimensionless form of the conservation equations is obtained using the following scales: d^* for length, d^{*2}/ν for time, ν/d^* for velocity, and $(\rho_0\nu^2)/d^{*2}$ for pressure, ν being the kinematic viscosity. The temperature and concentration differences $(T - T_0)$ and $(S - S_0)$, are scaled by $\Delta T = T_{\mathrm{u}} - T_{\mathrm{b}}$ and $\Delta S = S_{\mathrm{u}} - S_{\mathrm{b}}$, respectively. If $\mathbf{u}$ represents the dimensionless velocity vector, the set of conservation equations takes the form

$$\nabla \cdot \mathbf{u} = \mathbf{0} \tag{1}$$

$$\frac{\partial}{\partial t}\left(\frac{\mathbf{u}}{\phi}\right) + \frac{1}{\phi}\left(\mathbf{u} \cdot \nabla \frac{\mathbf{u}}{\phi}\right) = \nabla \cdot \left(\frac{1}{\phi}\nabla \mathbf{u} - P\mathbf{I}\right) - \frac{1}{Da}\mathbf{u} + Gr_{\mathrm{T}} T \mathbf{e}_z + Gr_{\mathrm{S}} S \mathbf{e}_z \tag{2}$$

$$\frac{\partial T}{\partial t} + \mathbf{u} \cdot \nabla T = \frac{1}{Pr_{\mathrm{f}}} \nabla \cdot \left(\frac{\alpha_{\mathrm{T}}}{\alpha_{\mathrm{Tf}}} \nabla T\right) \tag{3}$$

$$\phi \frac{\partial S}{\partial t} + \mathbf{u} \cdot \nabla S = \frac{1}{Sc_{\mathrm{f}}} \nabla \cdot (\phi \nabla S) \tag{4}$$

where $Gr_{\mathrm{T}} = (\rho_0 g \beta_{\mathrm{T}} \Delta T d^{*3})/\nu^2$ and $Gr_{\mathrm{S}} = (\rho_0 g \beta_{\mathrm{S}} \Delta S d^{*3})/\nu^2$ are the thermal and solutal Grashof numbers based on the total depth of the channel d and $Pr_{\mathrm{f}} = \nu/\alpha_{\mathrm{Tf}}$ and $Sc_{\mathrm{f}} = \nu/D_{\mathrm{f}}$ are the fluid Prandtl and Schmidt numbers (D_{f} being the molecular diffusivity), respectively. In the solute transport Eq. 4, due to absence of mass diffusion in the solid phase, the

effective solute diffusion coefficient in the absence of dispersion effect has been taken such that $D_{\text{eff}} = \phi D_{\text{f}}$ where ϕ represents the porosity.

In the momentum Eq. 2 $Da = K/d^{*2}$ is the Darcy number (dimensionless permeability) while the reduced viscosity in the Brinkman term has be taken such that $\mu_{\text{eff}}/\mu_{\text{f}} = 1/\phi$ (Whitaker 1999). The second Brinkman correction term has been neglected. Finally, α_{T} in Eq. 3 is the thermal diffusivity ($\alpha_{\text{T}} = \alpha_{\text{Tf}}$ in the fluid and $\alpha_{\text{T}} = \alpha_{\text{Tm}}$ in the porous region). The associated dimensionless boundary conditions at the external walls are

$$\begin{aligned} &\mathbf{u}(1) = \mathbf{u}(0) = \mathbf{0}, \quad T(1) = \frac{T_{\text{u}}^* - T_0^*}{\Delta T^*}, \quad T(0) = \frac{T_{\text{b}}^* - T_0^*}{\Delta T^*} \\ &S(1) = \frac{S_{\text{u}}^* - S_0^*}{\Delta S^*}, \quad S(0) = \frac{S_{\text{b}}^* - S_0^*}{\Delta S^*} \end{aligned} \tag{5}$$

In Eqs. 1–4 let us recall that the effective properties (ϕ, Da, and α_T) are Heaviside functions and therefore their differentiation must be considered in the meaning of the distributions (Schwartz 1961; Kataoka 1986).

3 Linear Stability Analysis

The perturbation equations are obtained in a usual way using the general decomposition

$$\zeta = \overline{\zeta}(z) + \zeta'(x, z, t) \tag{6}$$

where the overlined and prime notations represent the basic state and the perturbation of a generic variable ζ, respectively. The basic state is assumed to be quiescent and therefore $\overline{u}(z) = \overline{w}(z) = 0$ and $\partial/\partial t = 0$. For conciseness, basic states for the temperature and concentration are provided in Appendix. Equation 6 is introduced in Eqs. 1–5 and the resulting system is linearized. Assuming that the principle of exchange of stability holds, the linearized system gives

$$\begin{aligned} \frac{\partial}{\partial t}\left(\frac{\partial}{\partial z}\left(-\frac{1}{\phi}\frac{\partial w'}{\partial z}\right) + \frac{1}{\phi}\left(\frac{\partial^2 w'}{\partial x^2}\right)\right) = {} & \frac{\partial}{\partial z}\left(\frac{1}{Da}\right)\frac{\partial w'}{\partial z} + \frac{1}{Da}\frac{\partial^2 w'}{\partial x^2} + \frac{1}{Da}\frac{\partial^2 w'}{\partial z^2} \\ & - \frac{1}{\phi}\nabla^2\left(\frac{\partial^2 w'}{\partial x^2} + \frac{\partial^2 w'}{\partial z^2}\right) - \frac{\partial}{\partial z}\left(\frac{1}{\phi}\right)\nabla^2\left(\frac{\partial w'}{\partial z}\right) \\ & - \frac{\partial}{\partial z}\left(\frac{1}{\phi}\right)\frac{\partial^3 w'}{\partial z^3} - \frac{\partial^2}{\partial z^2}\left(\frac{1}{\phi}\right)\frac{\partial^2 w'}{\partial z^2} \\ & - \frac{\partial}{\partial z}\left(\frac{1}{\phi}\right)\frac{\partial^3 w'}{\partial x^2 \partial z} + Gr_{\text{T}}\frac{\partial^2 T'}{\partial x^2} + Gr_{\text{S}}\frac{\partial^2 S'}{\partial x^2} \end{aligned} \tag{7}$$

Similarly, the linearized energy and solutal Eqs. 3, 4 take the form

$$Pr_{\text{f}}\left(\frac{\partial T'}{\partial t} + w'\frac{\partial \overline{T}}{\partial z}\right) = \frac{\alpha_{\text{T}}}{\alpha_{\text{Tf}}}\left(\frac{\partial^2 T'}{\partial x^2} + \frac{\partial^2 T'}{\partial z^2}\right) + \frac{1}{\alpha_{\text{Tf}}}\frac{\partial \alpha_{\text{T}}}{\partial z}\frac{\partial T'}{\partial z} \tag{8}$$

$$Sc_{\text{f}}\left(\frac{\partial S'}{\partial t} + w'\frac{\partial \overline{S}}{\partial z}\right) = \phi\left(\frac{\partial^2 S'}{\partial x^2} + \frac{\partial^2 S'}{\partial z^2}\right) + \frac{\partial \phi}{\partial z}\frac{\partial S'}{\partial z} \tag{9}$$

According to the normal mode expansion, the vertical velocity component and the temperature and concentration are decomposed under the form

$$(w', T', S') = (W(z), \theta(z), \mathcal{S}(z))\, e^{i\kappa x + \sigma t} \tag{10}$$

with $\nabla_2^2 f + \kappa^2 f = 0$ ($\nabla_2^2 = \partial^2/\partial x^2$) and where $W(z)$, $\theta(z)$ and $\mathcal{S}(z)$ are the amplitudes of the velocity, temperature, and concentration, respectively. κ is the dimensionless wave number and σ is the complex growth rate. Assuming that the principle of exchange of stability holds ($\sigma = 0$) and introducing Eq. 10 into the linearized system gives

$$\begin{aligned}
&\frac{1}{\phi}\left(\frac{\mathrm{d}^4 W}{\mathrm{d}z^4} + \kappa^4 W\right) - \kappa^2\left(\frac{2}{\phi}\frac{\mathrm{d}^2 W}{\mathrm{d}z^2} - \frac{1}{Da}W + 2\frac{\mathrm{d}}{\mathrm{d}z}\left(\frac{1}{\phi}\right)\frac{\mathrm{d}W}{\mathrm{d}z}\right) \\
&\quad - \left(2\frac{\mathrm{d}}{\mathrm{d}z}\left(\frac{1}{\phi}\right)\frac{\mathrm{d}^3 W}{\mathrm{d}z^3} - \frac{\mathrm{d}}{\mathrm{d}z}\left(\frac{1}{Da}\right)\frac{\mathrm{d}W}{\mathrm{d}z} - \left(\frac{1}{Da} - \frac{\mathrm{d}^2}{\mathrm{d}z^2}\left(\frac{1}{\phi}\right)\right)\frac{\mathrm{d}^2 W}{\mathrm{d}z^2}\right) \\
&\quad + \kappa^2\left(Gr_\mathrm{T}\theta + Gr_\mathrm{S}\mathcal{S}\right) = 0 \qquad (11)
\end{aligned}$$

$$Pr_\mathrm{f}\left(\frac{\mathrm{d}\overline{T}}{\mathrm{d}z}W\right) = \frac{\alpha_\mathrm{T}}{\alpha_\mathrm{Tf}}\left(-\kappa^2\theta + \frac{\mathrm{d}^2\theta}{\mathrm{d}z^2}\right) + \frac{1}{\alpha_\mathrm{Tf}}\frac{\mathrm{d}\alpha_\mathrm{T}}{\mathrm{d}z}\frac{\mathrm{d}\theta}{\mathrm{d}z} \qquad (12)$$

$$Sc_\mathrm{f}\phi\left(\frac{\mathrm{d}\overline{S}}{\mathrm{d}z}W\right) = \phi\left(-\kappa^2\mathcal{S} + \frac{\mathrm{d}^2\mathcal{S}}{\mathrm{d}z^2}\right) + \frac{\mathrm{d}\phi}{\mathrm{d}z}\frac{\mathrm{d}\mathcal{S}}{\mathrm{d}z} \qquad (13)$$

The boundary conditions at the external walls take the form:

$$\begin{aligned}
&\theta(1) = 0, \quad \mathcal{S}(1) = 0, \ W(1) = 0, \quad \frac{\mathrm{d}W(1)}{\mathrm{d}z} = 0 \\
&\theta(0) = 0, \quad \mathcal{S}(0) = 0, \ W(0) = 0, \quad \frac{\mathrm{d}W(0)}{\mathrm{d}z} = 0
\end{aligned} \qquad (14)$$

The system given by Eqs. 11–14 represents the eigenvalue problem. It is solved using the GITT (Cotta 1993) and the critical Grashof is obtained by minimization over κ. For the sake of conciseness, the GITT is not described in this article and details concerning its application to such a fluid-porous configuration can be found in previous papers (Hirata et al. 2006; Hirata et al. 2007b). This numerical integral method has been validated by comparison with the exact values obtained in full fluid and porous cavities (Chandrasekhar 1961).

4 Numerical Results

In this section, the onset of natural convection due to thermal and solutal buoyancy forces is analyzed. First, the validation of the analysis is obtained by comparison of the numerical results to the exact values of Rayleigh-Bénard problem both in a pure fluid ($Da \to \infty, \phi = 1$) and in a full porous layer ($\widehat{d} = d_\mathrm{f}^*/d_\mathrm{m}^* \to 0$). As expected, in both cases, the marginal stability curves plotted in the plane (Ra_T, Ra_S) is a straight line (Nield and Bejan 1992). Here, the thermal and the solutal Rayleigh numbers are defined by $Ra_\mathrm{T} = Gr_\mathrm{T} Pr_\mathrm{f} Da$ and $Ra_\mathrm{S} = Gr_\mathrm{S} Sc_\mathrm{f} Da$, respectively. According to the boundary conditions given by Eq. 5, the fluid case leads to $-Ra_\mathrm{Tf} + Ra_\mathrm{Sf} = 1707.77$ with the associated wave number $\kappa = 3.12$. The full porous configuration leads to $-Ra_\mathrm{Tm} + Ra_\mathrm{Sm} = 4\pi^2 \approx 39.48$, with $\kappa = \pi \approx 3.14$. From the definitions $\Delta T = T_\mathrm{u} - T_\mathrm{b}$ and $\Delta\mathcal{S} = \mathcal{S}_\mathrm{u} - \mathcal{S}_\mathrm{b}$, it is possible to identify the regions where the temperature and concentration gradients are stabilizing or destabilizing (see, Figs. 2, 3). One verifies that the curves $Ra_\mathrm{S} \times Ra_\mathrm{T}$ obtained with this analysis are straight lines that crosses the axes in (0, 1707.77); (−1707.77, 0) and (0, 39.48); (−39.48, 0). All the results presented here have been obtained with the following parameters: $Pr_\mathrm{f} = 10$, $Da = 10^{-5}$, $\phi = 0.39$, and $\varepsilon_\mathrm{T} = \alpha_\mathrm{Tf}/\alpha_\mathrm{Tm} = 1$ (unless otherwise specified).

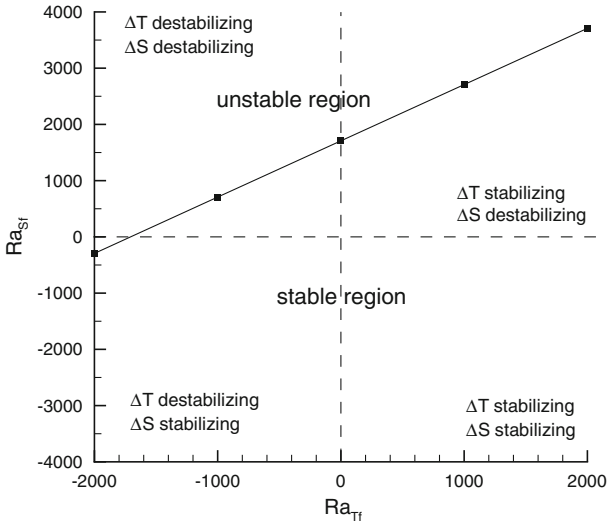

Fig. 2 Critical solutal Rayleigh number as a function of the thermal Rayleigh number for a full fluid layer ($Da \to \infty, \phi = 1$)

Fig. 3 Critical solutal Rayleigh number as a function of the thermal Rayleigh number for a full porous layer ($\widehat{d} \to 0$)

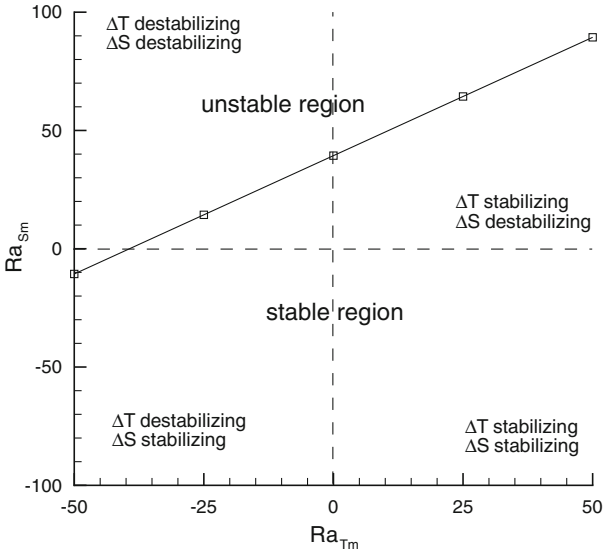

Figure 4 shows the stability curves obtained for different values of the depth ratio $\widehat{d}$. $Ra_T = 0$ and $Ra_S = 0$ correspond to the pure solutal or thermal cases, respectively. It is shown that as Ra_T increases (the thermal buoyancy forces are more stabilizing) higher concentration gradients are needed to destabilize the system. Contrary to the above limiting cases, the evolution of the stability curves are not straight lines for $Ra_T \geq 0$. This change can be explained by representing the critical wave number κ as a function of the thermal Rayleigh number Ra_T (Fig. 5). Two regions are clearly identified: for negative values of Ra_T, the critical mode corresponds to convection cells at large wave numbers while the critical mode for $Ra_T \geq 0$

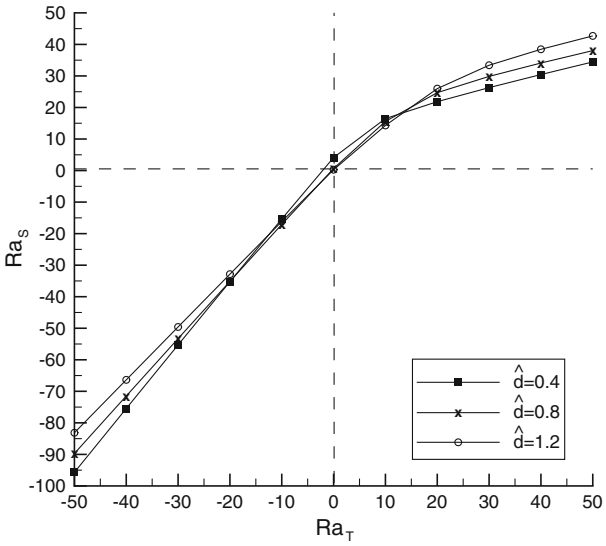

Fig. 4 Critical solutal Rayleigh number versus the thermal Rayleigh number, for three values of the depth ratio $\widehat{d}$

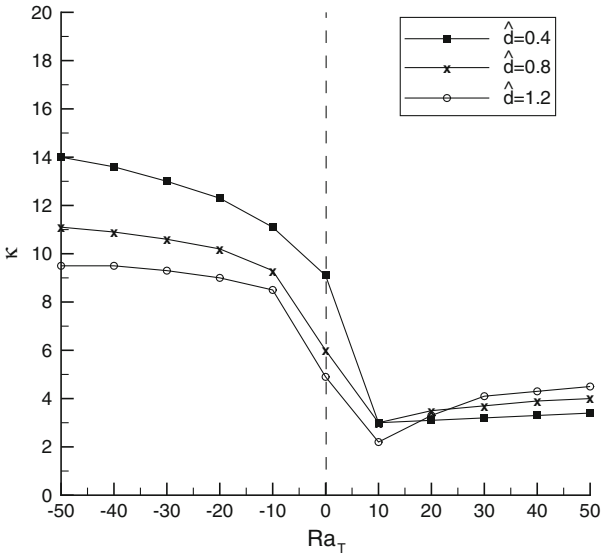

Fig. 5 Wave number versus the thermal Rayleigh number, for three values of the depth ratio $\widehat{d}$

corresponds to cells at small wave numbers. These results indicate that the bimodal nature of the marginal stability curves obtained for the pure thermal convection case (Chen and Chen 1988; Hirata et al. 2006) is also present in the thermosolutal case.

At small wave numbers the convective flow takes place in the whole cavity ("porous mode") while perturbations of large wave numbers lead to a convective flow mainly confined in the fluid layer ("fluid mode"). The streamline patterns and the vertical velocity profiles for $\widehat{d} = 0.8$ and different values of Ra_T are presented in Fig. 6a–d. Contrary to the pure thermal case where a single convection cell is observed, the onset of the thermosolutal case is

characterized by a multi-cellular regime for $Ra_T \ll 0$. This change is illustrated in Figs. 6a b. Indeed, for $Ra_T = -20$ (Fig. 6a), three contrarotating cells are present in the fluid region while the velocity field in the porous region is close to zero. When Ra_T increases, the wave length of the cell also increases (the wave number decreases) and at $Ra_T = 0$ (Fig. 6b) a monocellular flow is obtained (pure solutal case). For $Ra_T = +20$ (Fig. 6c) the flow starts to penetrate in the porous medium to finally occupy more or less the whole cavity for $Ra_T = +50$ (Fig. 6d).

Let us note that the multi-cellular regime of the thermosolutal case, had been already observed by Chen and Chen (Chen and Chen 1988) using a two-domain approach. Zhao and Chen (Zhao and Chen 2001) also have observed this type of multi-cellular structures using a one-domain model but they were not able to capture the two convective modes. It seems to us that one of the possible reasons for this difference is due to the fact that the differentiation of the discontinuous functions at the interface was not taken in the sense of distributions. In addition, in both studies, only one value of the thermal Rayleigh number was considered ($Ra_T \sim 50$).

Finally, the influence of the thermal diffusivity ratio

$$\varepsilon_T = \frac{\alpha_{Tf}}{\alpha_{Tm}} \tag{15}$$

for $\widehat{d} = 0.8$ is presented in Fig. 7. It is shown that a lower value of ε_T leads to a more unstable situation whatever the thermal Rayleigh number. As expected, in the absence of thermal buoyancy forces ($Ra_T = 0$) ε_T has no influence on the stability of the system. Moreover, it can be seen that the differences between the curves obtained for $\varepsilon_T = 0.7$ and 1 increases with $|Ra_T|$. The marginal stability curves (Ra_S versus κ) for two different values of Ra_T are presented in Figs. 8 and 9. For $Ra_T = -20$ (the temperature gradient is destabilizing) and $\varepsilon_T = 1$, it is important to remember that the convective flow is confined in the fluid region (see the streamline patterns on Fig. 6a). For $\varepsilon_T < 1$ heat diffusion is easier in the porous medium, and therefore the temperature at the interface increases. Under these circumstances, the temperature gradients in the fluid become more important, giving rise to a smaller value of the critical solutal Rayleigh number (Fig. 8). On the other hand, for $Ra_T = 20$ Fig. 9 shows that the critical mode is obtained for small wave numbers ("porous mode"). It is observed that decreasing ε_T hardly destabilizes the "porous mode" while the "fluid mode" (large wave numbers) is found to be more stable. This behavior can be explained by the stabilizing effect of the temperature gradient.

5 Conclusion

A linear stability analysis of thermosolutal natural convection in superposed fluid and porous layers has been carried out, using a one-domain model. It has been shown that the two convection modes observed in the pure thermal case are also present when thermosolutal convection is considered. In that case, it has been observed that the thermal Rayleigh number plays a fundamental role. Contrary to the pure thermal case where a single convection cell is observed, the onset of the thermosolutal case is characterized by a multi-cellular regime for $Ra_T \ll 0$. The analysis shows the moderate influence of the depth ratio. It also emphasizes the destabilizing influence of the thermal diffusivity ratio.

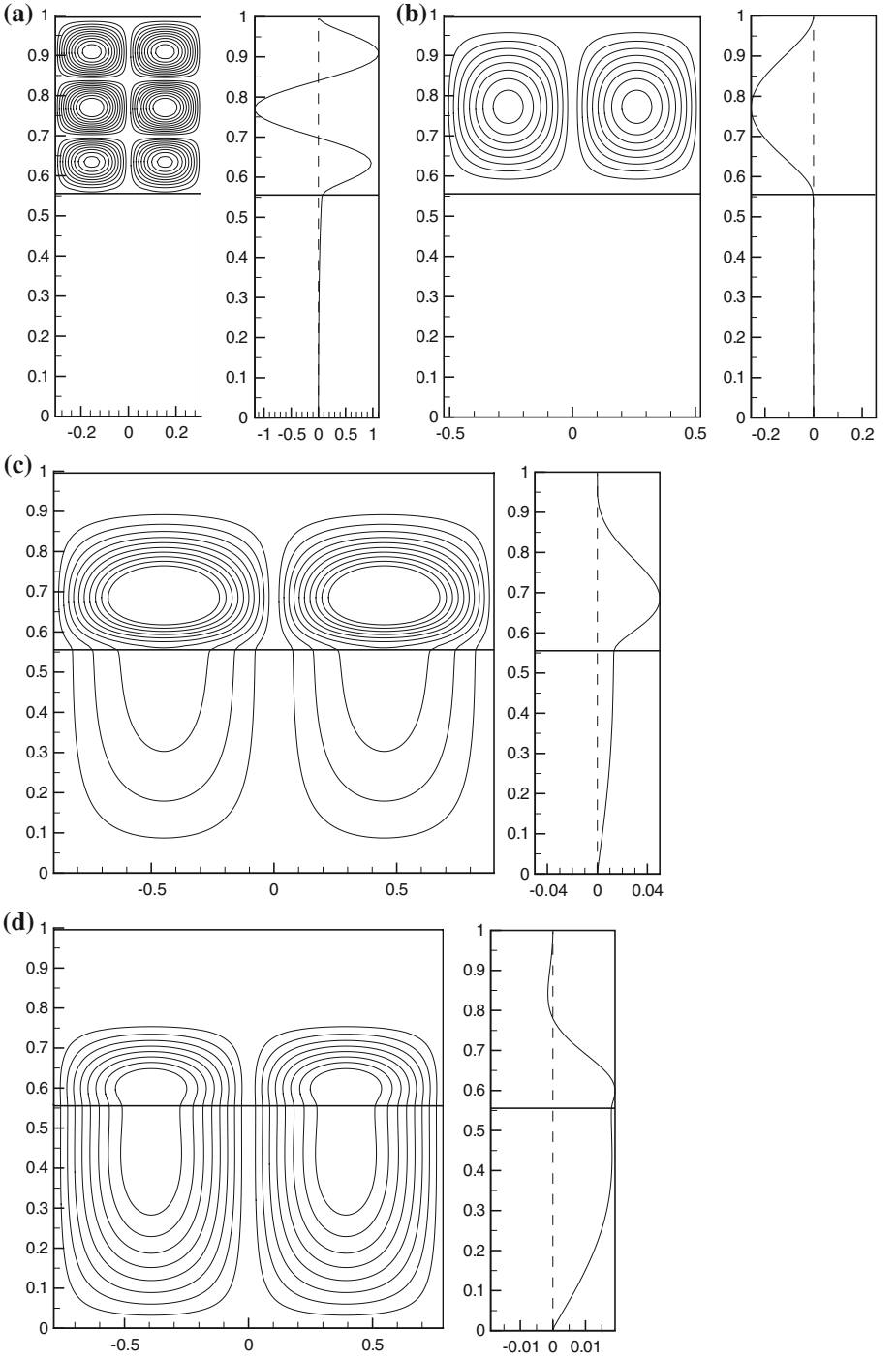

Fig. 6 Streamline patterns and vertical velocity profiles for $\widehat{d} = 0.8$: (**a**) $Ra_{\mathrm{T}} = -20$, $Ra_{\mathrm{S}} = -35.1$ and $\kappa_{cr} = 10.2$; (**b**) $Ra_{\mathrm{T}} = 0$, $Ra_{\mathrm{S}} = 0$ and $\kappa_{cr} = 6.0$; (**c**) $Ra_{\mathrm{T}} = 20$, $Ra_{\mathrm{S}} = 24.7$ and $\kappa_{cr} = 3.5$; (**d**) $Ra_{\mathrm{T}} = 50$, $Ra_{\mathrm{S}} = 38$ and $\kappa_{cr} = 4.0$. The thick horizontal line represents the fluid/porous interface

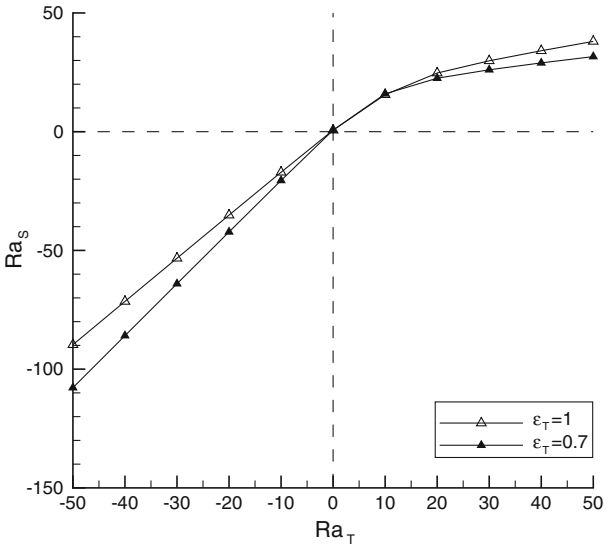

Fig. 7 Influence of the thermal diffusivity ratio ε_T for $\widehat{d} = 0.8$ and different thermal Rayleigh numbers

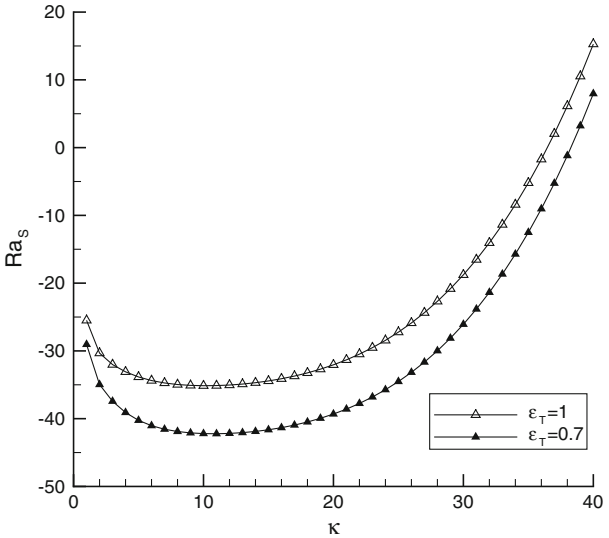

Fig. 8 Marginal stability curves obtained for two different values of the thermal diffusivity ratio ε_T, $\widehat{d} = 0.8$, $Ra_T = -20$

Appendix

Basic state for temperature and concentration

The basic state for the temperature in both the fluid and porous layers are given by

$$\overline{T}_{\mathrm{f}} = \frac{c_1}{\alpha_{\mathrm{Tf}}} z + c_2 \tag{16}$$

$$\overline{T}_{\mathrm{m}} = \frac{c_3}{\alpha_{\mathrm{Tm}}} z + c_4 \tag{17}$$

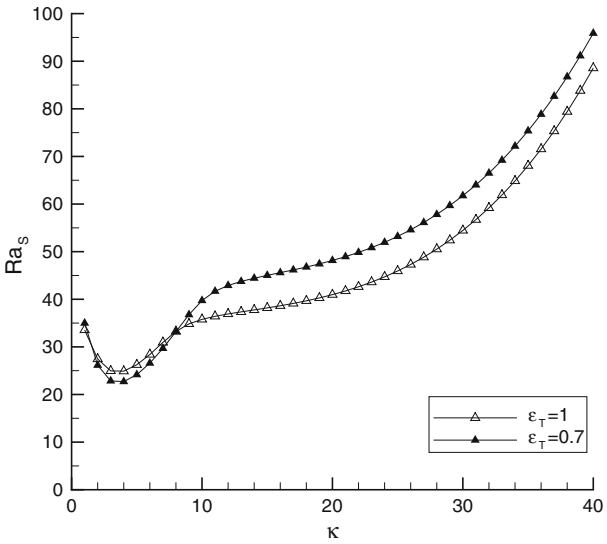

Fig. 9 Marginal stability curves obtained for two different values of the thermal diffusivity ratio ε_T, $\hat{d} = 0.8$, $Ra_T = +20$

with

$$c_1 = c_3 = \frac{\alpha_{Tm}\,\alpha_{Tf}(1+\hat{d})}{\hat{d}\,\alpha_{Tm} + \alpha_{Tf}} \tag{18}$$

$$c_2 = -\frac{\alpha_{Tm}(1+\hat{d})}{\hat{d}\,\alpha_{Tm} + \alpha_{Tf}} + \frac{T_u - T_0}{\Delta T} \tag{19}$$

$$c_4 = \frac{T_b - T_0}{\Delta T} \tag{20}$$

Similarly the basic state for the concentration takes the form

$$\overline{\mathcal{S}}_f = c_5 z + c_6 \tag{21}$$

$$\overline{\mathcal{S}}_m = \frac{c_7}{\phi_0} z + c_8 \tag{22}$$

where ϕ_0 is the porosity value in the porous layer. The constants $c_5 - c_8$ are given by

$$c_5 = c_7 = \frac{\phi_0(1+\hat{d})}{\hat{d}\,\phi_0 + 1} \tag{23}$$

$$c_6 = -\frac{\phi_0(1+\hat{d})}{\hat{d}\,\phi_0 + 1} + \frac{\mathcal{S}_u - \mathcal{S}_0}{\Delta\mathcal{S}} \tag{24}$$

$$c_8 = \frac{\mathcal{S}_b - \mathcal{S}_0}{\Delta\mathcal{S}} \tag{25}$$

References

Arquis, E., Caltagirone, J.: Sur les conditions hydrodynamiques au voisinage d'une interface milieu fluide-milieu poreux: application à la convection naturelle. C. R. Acad. Sci. **299-II**, 1–4 (1984)

Beavers, G.S., Joseph, D.D.: Boundary conditions at a naturally permeable wall. J. Fluid Mech. **30**, 197–207 (1967)

Beavers, G.S., Sparrow, E.M., Magnuson, R.A.: Experiments on coupled parallel flows in a channel and a bounding porous medium. J. Basic Eng. **92**, 843–848 (1970)
Brinkman, H.C.: A calculation of the viscous force exerted by flowing fluid on a dense swarm of particles. Appl. Sci. Res. **A1**, 27–34 (1947)
Carr, M.: Penetrative convection in a superposed porous-medium-fluid layer via internal heating. J. Fluid Mech. **509**, 305–329 (2004)
Carr, M., Straughan, B.: Penetrative convection in a fluid overlying a porous layer. Adv. Water Res. **26**, 263–276 (2003)
Chandesris, M., Jamet, D.: Boundary conditions at a planar fluid-porous interface for a Poiseuille flow. Int. J. Heat Mass Transf. **49**, 2137–2150 (2006)
Chandrasekhar, S.: Hydrodynamic and Hydromagnetic Stability. Oxford University Press, London (1961)
Chen, F., Chen, C.F.: Onset of finger convection in a horizontal porous layer underlying a fluid layer. J. Heat Transf. **110**, 403–409 (1988)
Cotta, R.M.: Integral Transforms in Computational Heat and Fluid Flow. CRC Press, Boca Raton (1993)
Goyeau, B., Lhuillier, D., Gobin, D., Velarde, M.G.: Momentum transport at a fluid-porous interface. Int. J. Heat Mass Transf. **46**(21), 4071–4081 (2003)
Hirata, S.C., Goyeau, B., Gobin, D., Cotta, R.M.: Stability in natural convection in superposed fluid and porous layers using integral transforms. Numer. Heat Transf. **50**(5), 409–424 (2006)
Hirata, S.C., Goyeau, B., Gobin, D.: Stability of natural convection in superposed fluid and porous layer: influence of the interfacial jump boundary condition. Phys. Fluids **19**, 058102 (2007a)
Hirata, S.C., Goyeau, B., Gobin, D., Carr, M., Cotta, R.M.: Stability analysis of natural convection in adjacent fluid and porous layer: influence of interfacial modeling. Int. J. Heat Mass Transf. **50**(7–8), 1356–1367 (2007b)
Hirata, S.C., Goyeau, B., Gobin, D., Chandesris, M., Jamet, D.: Stability of natural convection in superposed fluid and porous layers: equivalence of the one- and two-domain approaches. Int. J. Heat Mass Transf. **52**,533–536 (2009)
Kataoka, I.: Local instant formulation of two-phase flow. Int. J. Multiphase Flow **12**(5), 745–758 (1986)
Neale, G., Nader, W.: Practical significance of Brinkman's extension of Darcy's law: coupled parallel flow within a channel and a bounding porous medium. Can. J. Chem. Eng. **52**, 475–478 (1974)
Nield, D.A.: Onset of convection in a fluid layer overlying a layer of a porous medium. J. Fluid Mech. **81**, 513–522 (1977)
Nield, D.A.: The boundary correction for the Rayleigh-Darcy problem: limitations of the Brinkman equation. J. Fluid Mech. **128**, 37–46 (1983)
Nield, D., Bejan, A.: Convection in Porous Media. Springer-Verlag, New York (1992)
Ochoa-Tapia, J.A., Whitaker, S.: Momentum transfer at the boundary between a porous medium and a homogeneous fluid—I. Theoretical development. Int. J. Heat Mass Transf. **38**, 2635–2646 (1995a)
Ochoa-Tapia, J.A., Whitaker, S.: Momentum transfer at the boundary between a porous medium and a homogeneous fluid—II. Comparison with experiment. Int. J. Heat Mass Transf. **38**, 2647–2655 (1995b)
Schwartz, L.: Méthodes mathématiques pour les sciences physiques. Hermann, Paris (1961)
Whitaker, S.: The Method of Volume Averaging. Springer, New York (1999)
Zhao, P., Chen, C.F.: Stability analysis of double-diffusive convection in superposed fluid and porous layers using a one-equation model. Int. J. Heat Mass Transf. **44**, 4625–4633 (2001)